Journal of Applied Fluid Mechanics, Vol. 9, No. 4, pp. 1721-1730, 2016.
Available online at www.jafmonline.net, ISSN 1735-3572, EISSN 1735-3645.
DOI: 10.18869/acadpub.jafm.68.235.24422

Endoscopic Effects with Entropy Generation Analysis in Peristalsis for the Thermal Conductivity of $H_2O + Cu$ Nanofluid

N. S. Akbar [1], M. Raza [1†] and R. Ellahi [2,3]

[1] *DBS&H, CEME, National University of Sciences and Technology, Islamabad, Pakistan*

[2] *Department of Mathematics and Statistics, FBAS, IIU, Islamabad, 44000 Pakistan*

[3] *Department of Mechanical Engineering, Bourns Hall A 373, University of California Riverside CA 92521, USA*

†Corresponding Author Email: mohsin.phdma11@iiu.edu.pk

(Received December 25, 2014; accepted August 5, 2015)

ABSTRACT

The peristaltic flow of a copper water fluid investigate the effects of entropy and magnetic field in an endoscope is studied. The mathematical formulation is presented, the resulting equations are solved exactly. The obtained expressions for pressure gradient, pressure rise, temperature, velocity phenomenon entropy generation number and Bejan number are described through graphs for various pertinent parameters. The streamlines are drawn for some physical quantities to discuss the trapping phenomenon.

Keywords: MHD; Peristaltic flow; Copper nanoparticle; Endoscope; Entropy generation.

1. INTRODUCTION

Analysis of peristaltic flow has great practical importance and applications in many biological and biomedical systems. Such systems include the flow of urine through the ureter, the swallowing process through the oesophagus, the movement of spermatozoa in the ductus efferentes of the male reproductive tract, transport of lymph in the lymphatic vessels and in the vasomotion of small blood vessels such as arterioles, venules and capillaries. The literature on peristalsis of viscous fluid is by now quite extensive. Such relevant investigations include the works of Akbar *et al*. (2015), Mekheimer (2002), (2004), Akbar. (2014), Srinivas *et al*. (2009), Ebaid (2008 a, b), Akbar and Nadeem (2012). Misery *et al*. (2003) and Hakeem *et al*. (2002) talked about the effects of an endoscope on the peristaltic motion involving variable viscosity and generalized Newtonian fluids respectively.

Recently, Mekheimer and Elmaboud (2008) examined the peristaltic flow of couple stress fluid in an endoscope. According to them, the effects of an endoscope on the peristaltic fluid is very important for medical diagnosis, and it has many clinical applications, such as it is a very important tool for determining real reasons responsible for many problems in human organs in which the fluid are transported by peristaltic pumping (e.g., stomach small intestine). The endoscope is also like a catheter which is used in contemporary medical science. Some important studies to the topic were included in (2008, 2011)

The study of the peristaltic transport of a fluid in the presence of an external magnetic field and rotation is of great importance with regard to certain problems involving the movement of conductive physiological fluids, for example, blood and saline water. Pandey and Chaube (2011) investigated an analytical study of the MHD flow of a micropolar fluid through a porous medium induced by sinusoidal peristaltic waves traveling down the channel wall.

Li *et al*., (1994) have concluded that an impulsive magnetic filed in the combined therapy of patients with stone fragments in the upper urinary tract. It was discovered that the Impulsive Magnetic Field activates the impulsive activity of the uretaral smooth muscles in 100% of cases. Mekheimer and Al-Arabi (2002) investigated the non - linear peristaltic transport of MHD flow through a porous medium was studied in non - uniform channels.

It is also observed that heat transfer can be augmented through the improvement in the thermal properties of energy transmission fluids. If small solid particles in the fluid are suspended, then this might be an innovative way of improving the thermal conductivities of fluids. Nanofluids are estimated to show the conventional heat transfer fluids as comparing with superior heat transfer properties (2003). This idea of suspensions of colloidal particles dubbed as nanofluids was given by Choi (1995), he was at the view that small amounts of metallic or metallic oxide nanoparticles are dispersed into water and other fluids.

In thermodynamics, entropy is a measure of the number of specific ways in which a thermodynamic system may be arranged, often taken to be a measure of disorder, or a measure of progressing towards thermodynamic equilibrium. Non-Newtonian .fluid flow in a pipe system with entropy generation is considered by Pakdemirli and Yilbas (2006): According to them entropy number increases with increasing Brinkman number. Souidi *et al*. (2009) discussed entropy generation rate for a peristaltic pump. Entropy generation due to heat and fluid flow in backward facing step flow with various expansion ratios is studied by Abu-Nada (2006). Further analysis could be seen through Refs. (Koo and Kleinstreuer (2004, 2005), Oztop *et al*. (2004), Dagtekin *et al*. (2005,2007), Oztop and Al-Salem (2012), Ramiar *et al*. (2012), Ghasemi, and Razavi (2012), Rashad *et al*. (2013))

Motivated by the above analysis, the purpose of this study is to analyze the effect of peristaltic flow with entropy generation in heat conducting nanofluids in the presence of magnetic field in an endoscope. It is important to note that the analysis could be applied to any nanofluid, a copper-water nanofluid is used as the model in this article. We also consider thermal conductivity model with Brownian motion (Koo and. Kleinstreuer (2004)) for nanofluids, this gains the effects of particle size, particle volume fraction and temperature dependence. The analysis is performed under the well-established long wavelength and low Reynolds number approximations. The exact solution for the stream function, temperature and pressure gradient is given. All the physical features of the problems have been described with the help of graphs.

2. MATHEMATICAL FORMULATION

Here we discussed an incompressible peristaltic flow of copper nano fluid in an endoscope. The flow is generated by sinusoidal wave trains propagating with constant speed c along the walls of the tube. Heat transfer along with Entropy generation phenomena has been taken into account. The inner tube is rigid and maintained at temperature $\overline{T}_0$ while the outer tube has a sinusoidal wave traveling down its walls and maintained at temperature $\overline{T}_1$. The geometry of the wall surfaces is defined as

$$\overline{R_1} = a_1, \tag{1}$$

$$\overline{R_2} = a_2 + b\sin\left[\frac{2\pi}{\lambda}\left(\overline{Z} - c_1\overline{t}\right)\right]. \tag{2}$$

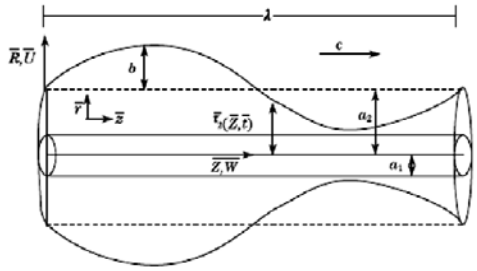

Fig. 1. Geometry of the problem.

In the above equations a_1 is the radius of the inner tube, a_2 is the radius of the outer tube at inlet, b is the wave amplitude, λ is the wavelength, c_1 he wave speed, and $\overline{t}$ the time. Introducing a wave frame $(\overline{r},\overline{z})$ moving with velocity c_1 away from the fixed frame $(\overline{R},\overline{Z})$ by the transformations

$$z = \overline{Z} - c_1\overline{t},\ r = \overline{R},\ w = \overline{W} - c_1,\ u = \overline{U} \tag{3}$$

$$\frac{1}{r}\frac{\partial\left(\overline{r}\overline{u}\right)}{\partial\overline{r}} + \frac{\partial\overline{w}}{\partial\overline{z}} = 0, \tag{4}$$

$$\begin{aligned}&\rho_{nf}\left(\overline{u}\frac{\partial\overline{u}}{\partial\overline{r}} + \overline{w}\frac{\partial\overline{u}}{\partial\overline{r}}\right) = -\frac{\partial\overline{P}}{\partial\overline{r}} + \\ &\mu_{nf}\left(\frac{\partial^2\overline{u}}{\partial\overline{r}^2} + \frac{1}{r}\frac{\partial\overline{u}}{\partial\overline{r}} + \frac{\partial^2\overline{u}}{\partial\overline{z}^2} - \frac{\overline{u}}{\overline{r}^2}\right),\end{aligned} \tag{5}$$

$$\begin{aligned}&\rho_{nf}\left(\overline{u}\frac{\partial\overline{w}}{\partial\overline{r}} + \overline{w}\frac{\partial\overline{u}}{\partial\overline{z}}\right) = -\frac{\partial\overline{P}}{\partial\overline{z}} + \\ &\mu_{nf}\left(\frac{\partial^2\overline{w}}{\partial\overline{r}^2} + \frac{1}{r}\frac{\partial\overline{w}}{\partial\overline{r}} + \frac{\partial^2\overline{w}}{\partial\overline{z}^2}\right) - \sigma B_0^2\left(\overline{w} + c_1\right),\end{aligned} \tag{6}$$

$$\begin{aligned}&\left(\overline{u}\frac{\partial\overline{T}}{\partial\overline{r}} + \overline{w}\frac{\partial\overline{T}}{\partial\overline{z}}\right) = \alpha_{nf}\left(\frac{\partial^2\overline{T}}{\partial\overline{r}^2} + \frac{1}{r}\frac{\partial\overline{T}}{\partial\overline{r}} + \frac{\partial^2\overline{T}}{\partial\overline{z}^2}\right) \\ &+ \frac{\mu_{nf}}{\left(\rho c_p\right)_{nf}}\left(\frac{\partial\overline{u}}{\partial\overline{r}} + \frac{\partial\overline{w}}{\partial\overline{r}}\right)^2,\end{aligned} \tag{7}$$

where $\overline{P}$ is the pressure the ambient value of temperature denoted by $\overline{T}_0$,$\overline{w}$ and $\overline{u}$ are the velocity components in the $\overline{r}$ and $\overline{z}$ directions, respectively, $\overline{T}$ is the local temperature of the fluid. Further, ρ_{nf} is the effective density, μ_{nf} is the effective dynamic viscosity, $\left(\rho c_p\right)_{nf}$ is the heat capacitance, α_{nf} is the effective thermal diffusivity, which are defined as (see Ref. Koo and Kleinstreuer 2004)

$$\begin{aligned}\rho_{nf} &= (1-\varphi)\rho_f + \varphi\rho_f, \\ \left(\rho c_p\right)_{nf} &= (1-\varphi)\left(\rho c_p\right)_f + \varphi\left(\rho c_p\right)_s, \\ (\rho\beta)_{nf} &= (1-\varphi)(\rho\beta)_f + \varphi(\rho\beta)_s.\end{aligned} \tag{8}$$

where subscript nf , f and s stand for the nanofluid, base fluid and nanoparticle, respectively and φ is the solid volume fraction, The corresponding boundary conditions in the wave frame are

$$\overline{w} = -c_1, \quad \overline{T} = \overline{T}_0, \quad \text{at } \overline{r} = \overline{r}_1, \tag{9}$$

$$\overline{w} = -c_1, \quad \overline{T} = \overline{T}_1, \quad \text{at } \overline{r} = \overline{r}_2 = a_2 + b\sin\frac{2\pi}{\lambda}\left(\overline{z}\right), \tag{10}$$

The dimensionless parameters used in the problem are defined as follow

$$R = \frac{\overline{R}}{a_2},\ r = \frac{\overline{r}}{a_2},\ Z = \frac{\overline{Z}}{\lambda},\ z = \frac{\overline{z}}{\lambda},\ W = \frac{\overline{W}}{c_1},\ w = \frac{\overline{w}}{c_1},$$
$$\mathrm{Re} = \frac{\rho c_1 c_2}{\mu_{nf}}, \delta = \frac{a_2}{\lambda},\ \overline{\theta} = \frac{T - T_0}{T_1 - T_0}, Br = Ec\,\mathrm{Pr};$$
$$\alpha_{nf} = \frac{k}{(\rho c)_f},\ t = \frac{c_1}{\lambda}\overline{t},\ \tau = \frac{(\rho c)_p}{(\rho c)_f},\ M^2 = \frac{\sigma B_o^2 a_2^2}{\mu_{nf}}$$

$$U = \frac{\lambda \overline{U}}{a_2 c_1},\ u = \frac{\lambda \overline{u}}{a_2 c_1},\ r_2 = \frac{\overline{r}_2}{a_2} = 1 + \omega\sin(2\pi z) \tag{11}$$

After using the above non-dimensional parameters and transformation in Eq. (2) employing the assumptions of long wavelength $(\delta \to 0)$, the dimensionless governing equations (without using bars) for nanofluid in the wave frame take the final form as

$$\frac{\partial u}{\partial r} + \frac{u}{r} + \frac{\partial w}{\partial z} = 0, \tag{12}$$

$$\frac{\partial p}{\partial r} = 0, \tag{13}$$

$$\frac{dp}{dz} = A * \frac{1}{r}\frac{\partial}{\partial r}\left(r\frac{\partial w}{\partial r}\right) - M^2(w+1), \tag{14}$$

$$Kf * \frac{1}{r}\frac{\partial}{\partial r}\left(r\frac{\partial \theta}{\partial r}\right) + B_r A * \left(\frac{\partial w}{\partial r}\right)^2 = 0, \tag{15}$$

The non-dimensional boundaries will take the form as

$$w = -1, \text{ at } \ r = r_1. \tag{16}$$

$$w = -1, \text{ at } \ y = r_2 = 1 + \omega\sin(2\pi z). \tag{17}$$

$$\theta = 0 \ \text{ at } r = r_1, \quad \theta = 1 \ \text{ at } r = r_2, \tag{18}$$

Eq. (7) are considered to be independent of the movement of nanoparticles. The Brownian motion is claimed to play an important role in modifying the thermal conductivity and viscosity of nanofluids. Among the existing models that predict the thermal conductivity and viscosity of nanofluids with considering the Brownian motion, the models proposed by Koo and Kleinstreuer (2004, 2005) are utilized in the present study. These models have successfully been used by Ghasemi and Aminossadati (2013) to study the effects of Brownian motion on laminar steady-state natural convection in a right triangular enclosure with localized heating on the vertical side. Note that these models were proposed based on water with copper oxide nanoparticles. Although the extension to other combinations of base liquids and nanoparticles may be justified, the material of the nanoparticles being considered in the present study are limited to copper only. In these models, it is assumed that the thermal conductivity and viscosity of nanofluids consist of two parts. One is referred to as the static part (k_s , μ_s) that is evaluated by mixture models, i.e., the Maxwell model for thermal conductivity and the Brinkman model for viscosity , and the other part (k_B , μ_B) is attributed to the Brownian motion. The expression for predicting the effective thermal conductivity of nanofluids appears as

$$k_{nf} = Kf + k_B. \tag{19}$$

where Kf is given by the

$$Kf = \frac{k_{nf}}{k_f} = \left(\frac{\dfrac{2k_s\,\varphi\log_{10}\left(\frac{k_f}{+}\right)}{k_s} - \varphi + 1}{\dfrac{2k_f\,\varphi\log_{10}\left(\frac{k_f}{+}\right)}{k_s} - \varphi + 1}\right). \tag{20}$$

and k_B is expressed as [22]

$$k_B = 5\times 10^4 \gamma_1 \varphi \left(\rho c_p\right)_f \sqrt{\frac{\kappa T_{env}}{\rho_s d_s}} F\left(T_{env}, \varphi\right), \tag{21}$$

where $\kappa\alpha$ is the Boltzmann constant and its value is $\kappa \approx 1.38\times 10^{-23} J/K$, d_s is the diameter of nanoparticles by assuming that these nanoparticles have a uniform size and are perfectly spherical i,e $d_s = 30nm$, T_{env} is a reference temperature that is chosen as T_0 in the current study, γ_1 is a function of the volume fraction φ of nanoparticles, which is given by

$$\gamma_1 = \begin{cases} 0.0137(100\varphi)^{-0.8229} & \text{for } \varphi < 0.01 \\ 0.0011(100\varphi)^{-0.7272} & \text{for } \varphi > 0.01 \end{cases}. \tag{22}$$

and the function $F\left(T_{env}, \varphi\right)$ is given by

$$\begin{aligned} F\left(T_{env}, \varphi\right) &= (-6.04\varphi + 0.4705)T_{env} \\ &+ (1722.3\varphi - 134.63), \end{aligned} \tag{23}$$

which is valid for $0.01 \le \varphi \le 0.04$ and $300K \le T_{env} \le 325K$.

We choose $T_{env} = 300K$ in the present study, for the expression for the thermal conductivity, the thermal diffusivity of nanofluids is then given by

$$\alpha_{nf} = \frac{k_{nf}}{\left(\rho c_p\right)_{nf}}. \tag{24}$$

The effective viscosity of nanofluids is given by

$$A = \mu_{nf} = \mu_s + \mu_B. \tag{25}$$

where μ_s is evaluated by Brinkman model

$$\mu_s = \mu_{nf}\left(1-\varphi\right)^{-2.5} \tag{26}$$

and μ_B is expressed as

$$\mu_B = 5\times 10^4 \gamma_1 \varphi \rho_{nf}\sqrt{\frac{\kappa T_{env}}{\rho_s d_s}}F\left(T_{env},\varphi\right). \tag{27}$$

The thermophysical properties, for pure water, copper are listed in Table 1 .

Table 1 Thermal physical properties of water and Nanoparticles

Physical Properties	Water H_2O	Copper Cu
ρ(kgm^{-3})	997.1	8933
Cp	4179	385
$\beta x10^5(K^{-1})$	21	1.67
$kxWm^{-1}(K^{-1})$	0.613	401

Entropy generation can be defined as follows (Pakdemirli and Yilbas 2006, Souidi *et al*. 2009)

$$S_G = \frac{k_{nf}}{T_0}\left(\left(\frac{\partial \overline{T}}{\partial \overline{r}}\right)^2+\left(\frac{\partial \overline{T}}{\partial \overline{z}}\right)^2\right) + \frac{\mu_{nf}}{T_0}\left(2\left(\left(\frac{\partial \overline{u}}{\partial \overline{r}}\right)^2+\left(\frac{\partial \overline{w}}{\partial \overline{z}}\right)^2\right)+\left(\frac{\partial \overline{w}}{\partial \overline{r}}+\frac{\partial \overline{u}}{\partial \overline{z}}\right)^2\right), \tag{28}$$

Dimensionless form of the Entropy Generation with the help of Eq. (10) due to fluid friction and magnetic field is given as:

$$N_s = \frac{S_G}{S_{G_0}} = \frac{k_{nf}}{k_f}\left(\frac{\partial \theta}{\partial r}\right)^2 + \Lambda Br\left(\frac{\partial w}{\partial r}\right)^2, \tag{29}$$

The dimensionless form of S_G is known as entropy generation number N_S which is the ratio of actual entropy generation rate to the characteristic entropy transfer rate S_{G_0} , which is defined as follows

$$S_{G_o} = \frac{k_f\left(T_1-T_0\right)^2}{T_0 a_2^2},\quad B_r = \frac{\mu_f c^2}{k_f\left(T_1-T_0\right)},\quad \Lambda = \frac{T_0}{\left(T_1-T_0\right)}. \tag{30}$$

Equation (28) consists of two parts. The first part is the entropy generation due to finite temperature difference (Nscond) and the second part is the entropy generation due to viscous effects (Nsvisc). The Bejan number is defined as (Nada, (2006))

$$B_e = \frac{Ns_{cond}}{Ns_{cond}+Ns_{visc}}. \tag{31}$$

3. SOLUTION OF THE PROBLEM

The exact solutions of the above equations are found as follows

$$w\left(r\right) = C_1 J_0\left(\frac{iMr}{\sqrt{A}}\right)+C_2 Y_0\left(-\frac{iMr}{\sqrt{A}}\right)-\frac{M^2+\frac{dp}{dz}}{M^2}, \tag{32}$$

where

$$C_1 = \frac{\frac{dp}{dz}\left(Y_0\left(-\frac{iMr1}{\sqrt{A}}\right)-Y_0\left(-\frac{iMr2}{\sqrt{A}}\right)\right)}{M^2\left(Y_0\left(-\frac{iMr1}{\sqrt{A}}\right)J_0\left(\frac{iMr2}{\sqrt{A}}\right)-J_0\left(\frac{iMr1}{\sqrt{A}}\right)Y_0\left(-\frac{iMr2}{\sqrt{A}}\right)\right)}. \tag{33}$$

$$C_2 = \frac{\frac{dp}{dz}\left(J_0\left(\frac{iMr1}{\sqrt{A}}\right)-J_0\left(\frac{iMr2}{\sqrt{A}}\right)\right)}{M^2\left(J_0\left(\frac{iMr1}{\sqrt{A}}\right)Y_0\left(-\frac{iMr2}{\sqrt{A}}\right)-Y_0\left(-\frac{iMr1}{\sqrt{A}}\right)J_0\left(\frac{iMr2}{\sqrt{A}}\right)\right)}. \tag{34}$$

$$\theta(y) = C_4 + \int_1^r\left(\frac{C_3}{K[2]}+\frac{\int_1^{K[2]}\frac{\left(BrC_1^2M^2K[1]J_1\left(\frac{iMK[1]}{\sqrt{A}}\right)^2 - 2BrC_1C_2M^2K[1]J_1\left(\frac{iMK[1]}{\sqrt{A}}\right)Y_1\left(-\frac{iMK[1]}{\sqrt{A}}\right)+ BrC_2^2M^2K[1]Y_1\left(-\frac{iMK[1]}{\sqrt{A}}\right)^2\right)}{Kf}dK[1]}{K[2]}\right)dK[2]. \tag{35}$$

$$\frac{dp}{dz} = \frac{\left(M\left(C_1Mr1^2\,{}_0\tilde{F}_1\left(2,\frac{M^2r1^2}{4A}\right)-C_1Mr2^2\,{}_0\tilde{F}_1\left(2,\frac{M^2r2^2}{4A}\right)+2F*M-Mr1^2+Mr2^2\right)+2iM\left(\sqrt{A}C_2r1Y_1\left(-\frac{iMr1}{\sqrt{A}}\right)-\sqrt{A}C_2r2Y_1\left(-\frac{iMr2}{\sqrt{A}}\right)\right)\right)}{r1^2-r2^2}. \tag{36}$$

The corresponding stream function can be defined as

$$u = -\frac{1}{r}\frac{\partial \psi}{\partial z} \text{ and } w = \frac{1}{r}\frac{\partial \psi}{\partial r}. \tag{37}$$

The pressure rise Δp is defined as follows

$$\Delta p = \int_0^1 \frac{dp}{dz}dz, \tag{38}$$

where the $\frac{dp}{dz}$ is defined in Eq.

The flow rate F in non dimonsionalized form is given as

$$F = 2Q - \frac{\omega^2}{2} - 1. \tag{39}$$

C_3, C_4 are constants and $K[1]$, $K[2]$

evaluated using Mathematica 9 .

4. RESULTS AND DISCUSSION

In this section we study the behavior of the solutions in the form of graphs, for several values，Hartmann number M , and volume flow rate Q has been carried out for both pure water and copper water. The variation of Q and M on pressure gradient is shown in Fig. 2, it shows that pressure gradient is decreasing on an increase in M for both types of fluid it is also observed that pressure gradient is least in case of copper water where as the effect of M is relatively larger in case of pure water.

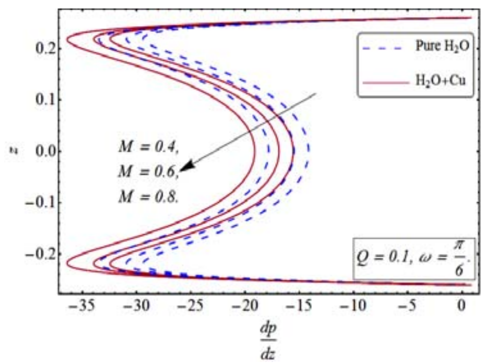

Fig. 2. Variation of pressure gradient dp/dz for different flow parameters.

In order to analyze pumping characteristics, numerical integration is performed and results are shown the variation of pressure rise per wavelength Δp against time average flux Q in Fig. 3. Fig.3 shows the effect of M on pressure rise, it is observed that pressure rise increases by increase in M in the region $(\Delta p > 0, Q > 0)$ while the opposite behavior is observed in the region $(\Delta p < 0, Q < 0)$. Figs. $4(a)-4(c)$ to understand the variation of temperature distribution for different values of φ, M and Br. Fig. $3(a)$ shows that θ increases as we increase φ for copper water fluid When we observe Figs. $4(b)$ and $4(c)$, the same trend is observed for Hartmann number M and Brinkmann number Br respectively, we have observed that by increasing M and Br, temperature is increasing.

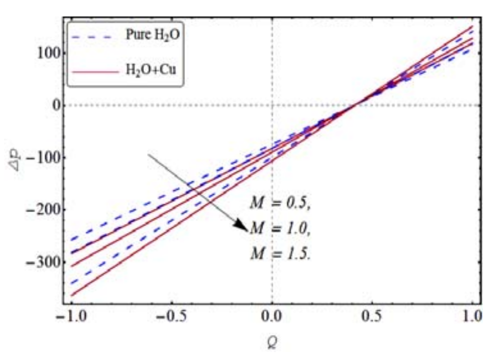

Fig. 3. Variation of pressure rise Δp for different flow parameters.

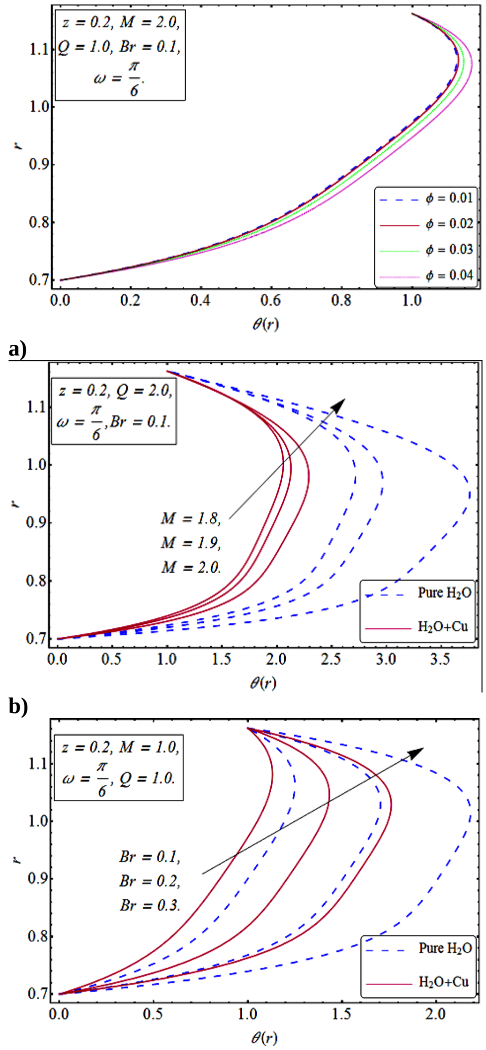

Fig. 4. Variation of temperature profile θ for different flow parameters.

We have plotted Fig. 5 to illustrate the effects of pertinent parameters on velocity profile w. It is observed from Fig. $5(a)$ that velocity profile increases with increase in the value of φ near the wall of tube $r2$. However, opposite behavior is shown near the wall $r1$. i.e. along with the sinusoidal wall, volume friction increases the velocity of fluid. We have presented the Figs.5 (b) to obtain the variation of velocity profile u for varying the magnitude of the parameters M for both types of fluid. It depicts that velocity is decreasing with increase of M along the wall $r2$, but opposite behavior is shown along the rigid tube's wall $r1$. Figs $5(c)$ show the variations of average flow rate Q on velocity profile it depicts that velocity increases with an increase in Q it is also observed that there is the least effect of Q on velocity in the case of copper water as compare to pure water.

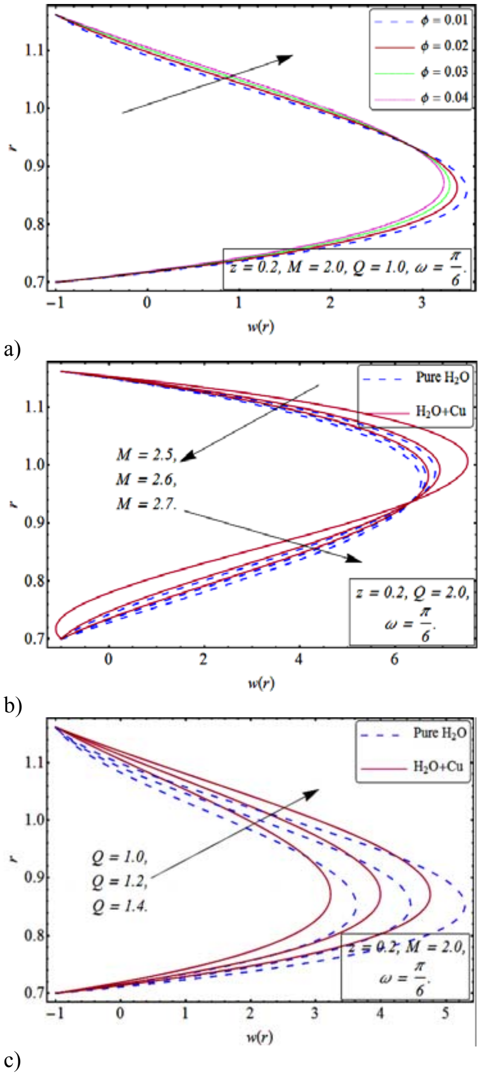

Fig. 5. Variation of velocity profile u with for different flow parameters.

We have presented the Fig. 6 to obtain the variation of entropy generation number N_s for varying the magnitude of the parameters φ, M, Br, and Λ. From Fig. $6(a)$ it depicts that N_s is increasing with increase nano particle volume friction parameter φ. Figs 6 (b) and 6 (c) shows that N_s is directly proportional to the M and Br throughout the channel but considerable impact is not observed along the walls for both types of fluid in case of Hartmann number and the impact of copper water is observed more than pure water. Nevertheless Fig 6 (d) shows the higher value of Λ displays least entropy.

Figs. $7(a)-7(d)$ are prepared to analyze the Bejan number with respect to change in different physical constraints involved. Fig. $8(a)$ depicts that with the increase in φ, there is a increase in Bejan number. Fig.7 (b) shows the variation of Bejan number for different values of M ， we see that near the wall $r2$ Bejan number is not influenced to considerable degree while near the wall $r1$ Bejan number is decreasing by increase in the values of M. Fig.7 (c) shows that there is an opposite behavior for Br as we see for M . We have observed in Fig. 8 (d) that B_e is increasing by increase in Λ but the impact on copper water is greater than the impact of pure water.

Another important phenomenon in peristaltic transport is trapping. The formation of an internally circulating bolus of fluid by closed streamlines is called trapping and is pushed a head along with the peristaltic wave. The physical phenomena may be responsible for thrombus formation in blood and the movement of food bolus in gastrointestinal tract. Fig. 8 show contour maps for the streamlines with four values of φ $(\varphi = 0.01, \varphi = 0.02, \varphi = 0.03, \varphi = 0.04)$ copper water. It is noticed that bolus becomes Smaller when we give greater values of φ.

Figs. 9 and 10 show the the effect of Hartmann number M on streamlines for pure water and copper water respectively it is shown that bolus becomes large as larger values of M. Figs. 11 and 12 show the effect of flow rate Q on streamlines for pure water and copper water respectively it is shown that bolus becomes large as larger values of Q.

5. CONCLUSION

Interaction of Copper nanoparticles for the peristaltic flow in endoscope with the magnetic field is discussed, key points are observed as follows:

1. It is observed that effect of nano particle friction on pressure gradient considerable impact i.e, more the volume friction, lesser the pressure gradient.

2. It is observed that temperature increases as we increase Brinkman number and Hartmann number for both types of fluid.

3. velocity is decreasing with increase of M along the sinusoidal wall , but opposite behavior is shown along the rigid tube's wall.

4. It is observed that Entropy generation number are increasing with increase of Brinkman number.

5. It is observed near the sinusoidal wall Bejan number is not influenced to considerable degree while near the rigid wall Bejan number is decreasing by increase in the values of Hartmann number.

6. It is noticed that size, of bolus becomes smaller when we give greater values of nano particle volume friction for copper water.

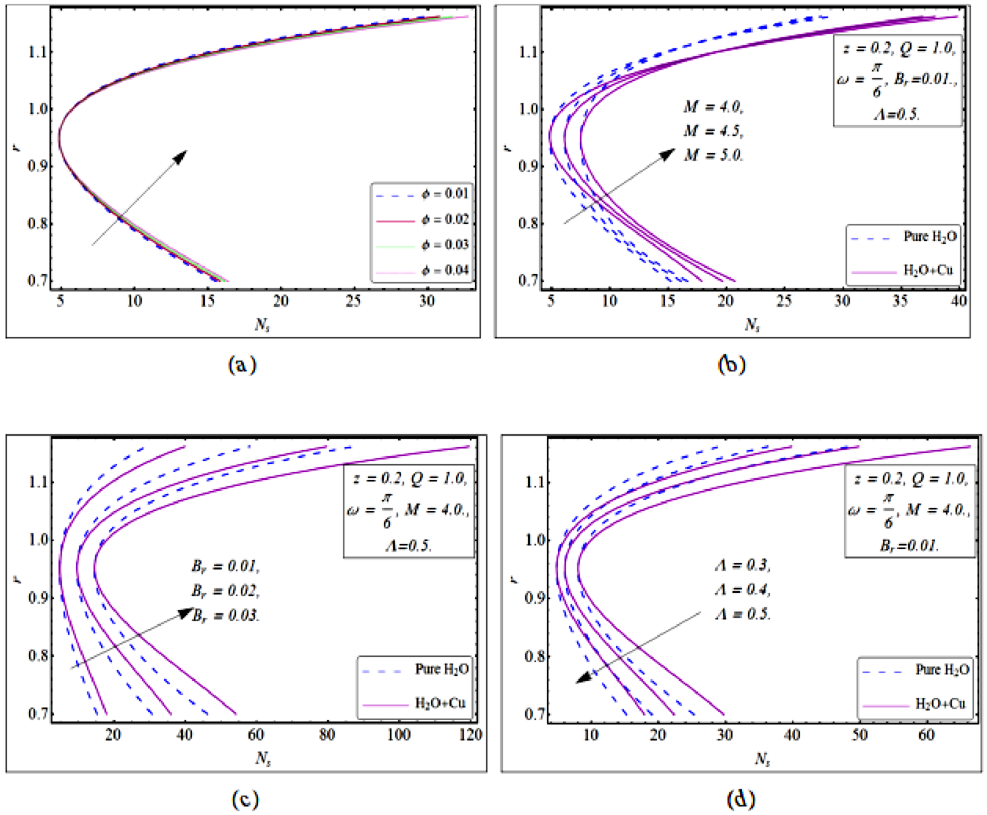

Figs . 6. Variation of entropy generation Ns for different flow parameters.

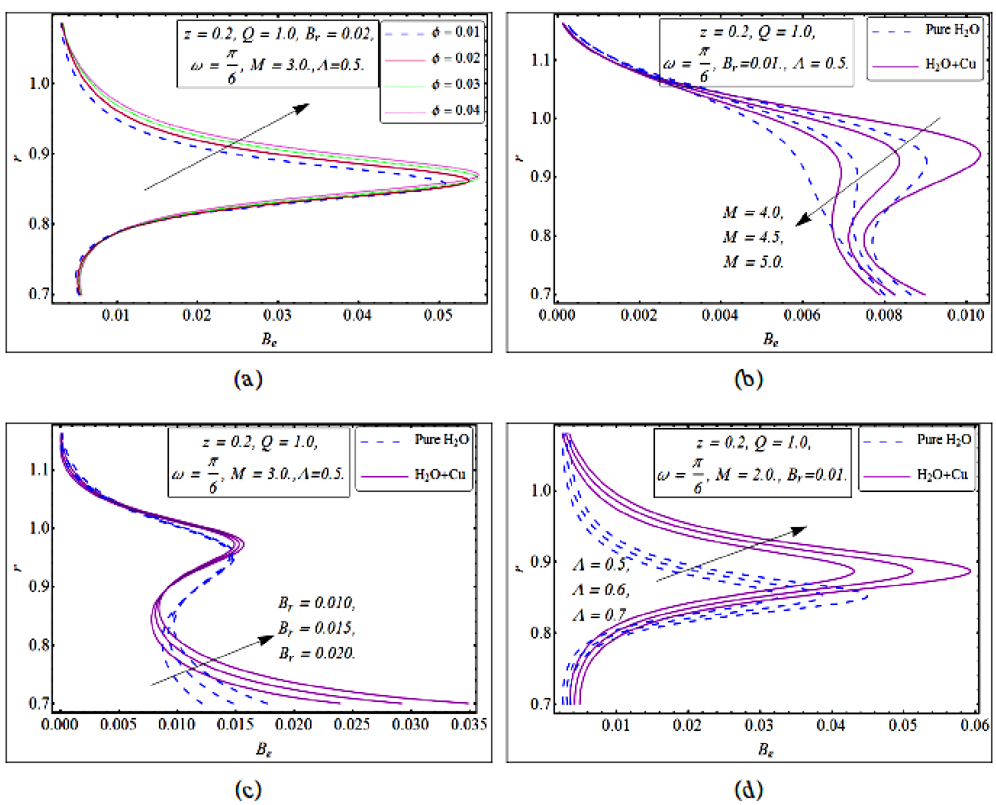

Fig. 7. Variation of Bejan number B_e with for different flow parameters.

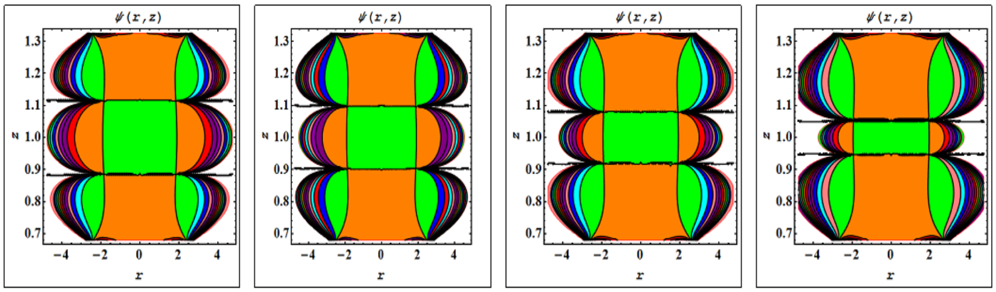

a **b** **c** **d**

Fig. 8. Stream lines of $H_2O + Cu$ **for different values of** φ. (a) **for** $\varphi = 0.01$, (b) **for** $\varphi = 0.02$, (c) **for** $\varphi = 0.03$, (d) **for** $\varphi = 0.04$. **The other parameters are** $Q = 1.0, M = 2.0, \omega = \frac{\pi}{6}$.

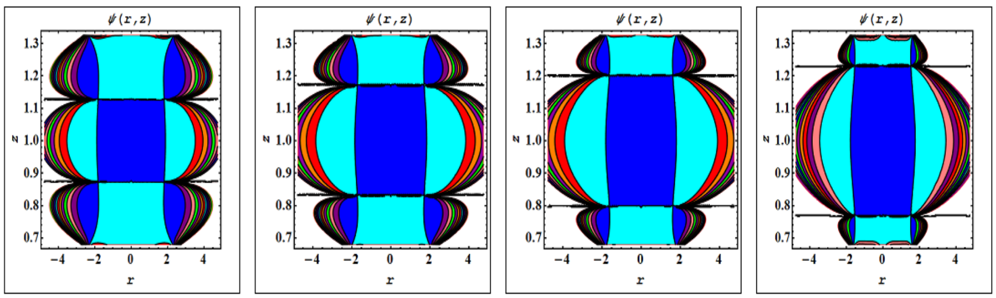

a **b** **c** **d**

Fig. 9. Stream lines of Pure H_2O **for different values of** M. (a) **for** $M = 2.0$, (b) **for** $M = 2.1$, (c) **for** $M = 2.2$, (d) **for** $M = 2.2$. **The other parameters are** $Q = 1.0, \omega = \frac{\pi}{6}$.

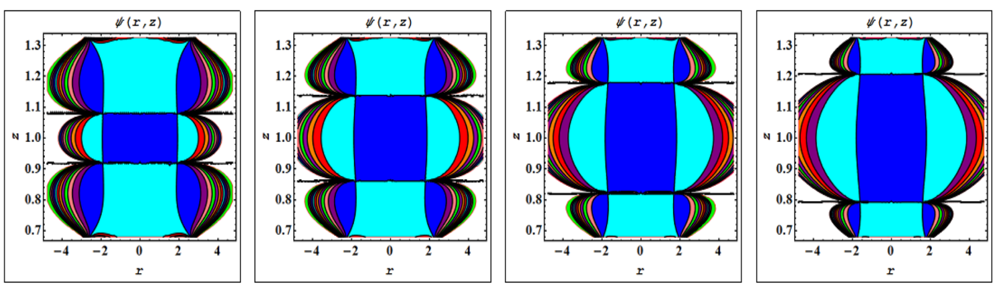

a **b** **c** **d**

Fig. 10. Stream lines of $H_2O + Cu$ **for different values of** M. (a) **for** $M = 2.0$, (b) **for** $M = 2.1$, (c) **for** $M = 2.2$, (d) **for** $M = 2.2$. **The other parameters are** $Q = 1.0, \omega = \frac{\pi}{6}$.

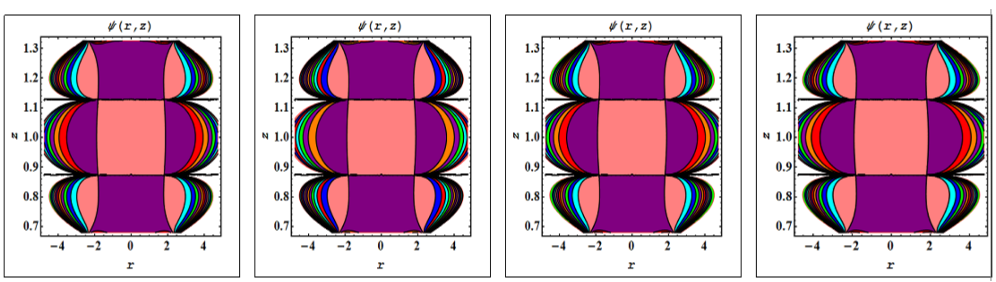

a **b** **c** **d**

Fig. 11. Stream lines of Pure H_2O **for different values of** Q. (a) **for** $Q = 1.0$, (b) **for** $Q = 1.5$, (c) **for** $Q = 2.0$, (d) **for** $Q = 2.5$. **The other parameters are** $M = 2.0, \omega = \frac{\pi}{6}$.

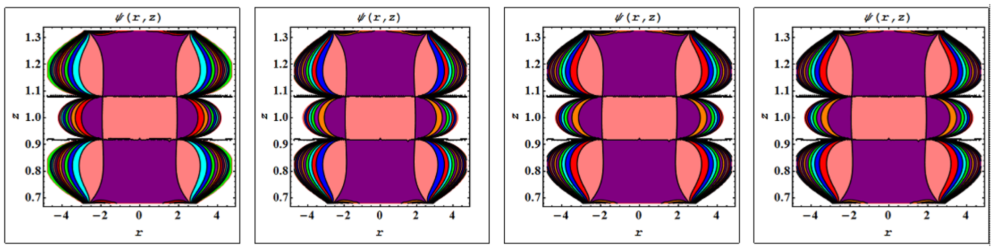

a b c d

Fig. 12. Stream lines of $H_2O + Cu$ **for different values of** Q. (a) **for** $Q = 1.0$, (b) **for** $Q = 1.5$, (c) **for** $Q = 2.0$, (d) **for** $Q = 2.5$. **The other parameters are** $M = 2.0, \omega = \frac{\pi}{6}$.

ACKNOWLEDGEMENT

Authors are thankful to the Higher Education Commission Pakistan for financial support to complete this work.

REFERENCES

Akbar, N. S. (2015). Application of Eyring-Powell fluid model in peristalsis with nano particles. *Journal of computational and theoretical nanosciences 12, 94-100.*

Akbar, N. S. (2014). Peristaltic flow of Cu-water nanofluid in a tube. *Journal of computational and theoretical nanosciences* 11, 1411 – 1416.

Akbar, N. S. and S. Nadeem (2011). Endoscopic effects on the peristaltic flow of a nanofluid, Commun. *Theor. Phys.* 56, 761 – 768.

Akbar, N. S., S. Nadeem, T. Hayat and A. A. Hendi (2012). Peristaltic flow of a nanofluid in a non-uniform tube. *Heat and Mass Transfer.* 48, 451 – 459.

Choi, S. U. S. (1995). Enhancing thermal conductivity of fluids with nanoparticle. *ASME Fluids Eng. Div. 231, 99-105.*

Dagtekin, I., H. F. Oztop and A. Bahloul (2007). Entropy Generation for Natural Convection in <GAMMA>-Shaped Enclosures. *Int. Comm. Heat Mass Transfer* 34, 502 – 510.

Dagtekin, I., H. F. Oztop, A. Z. Sahin (2005). An Analysis of Entropy Generation through Circular Duct with Different Shaped Longitudinal Fins of Laminar Flow. *Int. J. Heat Mass Transfer* 48(1), 171 – 181.

Ebaid, A. (2008). A new numerical solution for the MHD peristaltic flow of a bio-fluid with variable viscosity in a circular cylindrical tube via Adomian decomposition method. *Phys. Lett. A 372, 5321-5328.*

Ebaid, A. (2008). Effects of magnetic field and wall slip conditions on the peristaltic transport of a Newtonian fluid in an asymmetric channel. *Phys. Lett. A 372, 4493-4499.*

Ghasemi, J. and S. E. Razavi (2013). Numerical Nanofluid Simulation with Finite Volume Lattice-Boltzmann Enhanced Approach. *Journal of Applied Fluid Mechanics 6, 519-527.*

Hakeem, A. E., A. E. Naby and A. E. M. Misery (2002). Effects of an endoscope and generalized Newtonian fluid on peristaltic motion. *Applied Mathematics and Computation 128(1), 19-35.*

Jou, R. Y. and S. C. Tzeng (2006). Numerical research of nature convective heat transfer enhancement filled with nanofluids in rectangular enclosures. *Int. Commun. Heat Mass Transf. 33, 727-736.*

Koo, J. and C. Kleinstreuer (2004). A new thermal conductivity model for nanofluids. *J.Nanoparticle. 6, 577-588.*

Koo, J. and C. Kleinstreuer (2005). Laminar nanofluid flow in microheat-sinks. *Int. J. Heat Mass Transfer 48, 2652-2661.*

Li, A. A., N. I. Nesteron, S. N. Malikova and V. A. Kilatkin (1994). The use of an impulse magnetic field in the combined therapy of patients with stone fragments in the upper urinary tract. Vopr Kurortol Fizide. *Lech Fiz Kult. 3, 22-24.*

Mekheimer, Kh. S. (2002). Peristaltic transport of a couple-stress fluid in a uniform and non-uniform channels. *Biorheol. 39, 755-765.*

Mekheimer, Kh. S. (2004). Peristaltic flow of blood under effect of a magnetic field in a non uniform channels. *Appl. Math. Computation 153, 763-777.*

Mekheimer, K. S. and T. H. AL-Arabi (2003). Non-linear peristaltic transport of MHD flow through a porous medium. *Int. J. Maths. Sci. 26, 1663-1682.*

Mekheimer, Kh. S. and Y. A. Elmaboud (2008). Peristaltic flow of a couple stress fluid in an annulus: application of an endoscope. *Physica A 387, 2403-2415.*

Mekheimer, K. S. and Y. A. Elmaboud (2008). The influence of heat transfer and magnetic field on peristaltic transport of a Newtonian fluid in a vertical annulus: an application of an endoscope. *Physics Letters A 372, 1657-1665.*

Misery, E., A. M. Hakeem, A. E. Naby, A. E. and A. H. E. Nagar (2003). Effects of a fluid with variable viscosity and an endoscope on peristaltic motion. *Journal of the Physical Society of Japan 72(1), 89-93.*

Nada, E. A. (2006). Entropy generation due to heat and fluid flow in backward facing step flow with various expansion ratios. *Int. J. Exergy 3, 419-435.*

Oztop, H. F. and K. Al-Salem (2012). A Review on Entropy Generation in Natural and Mixed Convection Heat Transfer for Energy Systems. *Ren. Sust. En. Reviews* $16(1), 911-920$.

Oztop, H. F., A. Z. Sahin and I. Dagtekin (2004). Entropy Generation Through Hexagonal Cross-Sectional Duct for Constant Wall Temperature in Laminar Flow. *Int. J. Energy Res.* $28(8), 725-737$.

Pakdemirli, M. and B. S. Yilbas (2006). Entropy generation in a pipe due to non-Newtonian fluid flow: Constant viscosity case. *Sadhana* $31, 21-29$.

Pandey, S. K. and M. K. Chaube (2011). Peristaltic flow of a micropolar fluid through a porous medium in the presence of an external magnetic field. *Communications in Nonlinear Science and Numerical Simulation 16(9), 3591-3601.*

Ramiar, A., A. A. Ranjbar and S. F. Hosseinizadeh (2012). Effect of Axial Conduction and Variable Properties on TwoDimensional Conjugate Heat Transfer of Al2O3-EG/Water Mixture Nanofluid in Microchannel. *Journal of Applied Fluid Mechanics* $5, 79-87$.

Rashad, A. M. A. J. Chamkha and M. M. M. Abdou (2013). Mixed Convection Flow of Non-Newtonian Fluid from Vertical Surface Saturated in a Porous Medium Filled with a Nanofluid. *Journal of Applied Fluid Mechanics 6, 301-309.*

Souidi, F., K. Ayachi and N. Benyahia (2009). Entropy Generation Rate for a Peristaltic Pump. *J. Non-Equilib. Thermodyn. 34, 171–194.*

Srinivas, S., R. Gayathri and M. Kothandapani (2009). The influence of slip conditions, wall properties and heat transfer on MHD peristaltic transport. *Comput. Phys. Commun. 180, 2115-2122.*